JACS
JOURNAL OF THE AMERICAN CHEMICAL SOCIETY

ARTICLE

pubs.acs.org/JACS

Vibrational Density of States of Hydration Water at Biomolecular Sites: Hydrophobicity Promotes Low Density Amorphous Ice Behavior

Daniela Russo,[*,†] José Teixeira,[‡] Larry Kneller,[§,∥] John R. D. Copley,[§] Jacques Ollivier,[⊥] Stefania Perticaroli,[#] Eric Pellegrini,[⊥] and Miguel Angel Gonzalez[⊥]

[†]CNR-IOM c/o Institut Laue Langevin, 6 rue J. Horowitz BP156, F-38042 Grenoble, France

[‡]Laboratoire Léon Brillouin (CEA/CNRS), CEA Saclay, 91191 Gif-sur Yvette Cedex, France

[§]National Institute of Standards and Technology, Gaithersburg, Maryland 20899-6102, United States

[∥]Department of Materials Science and Engineering, University of Maryland, College Park, Maryland 20742, United States

[⊥]Institut Laue Langevin, 6 rue J. Horowitz BP156, F-38042 Grenoble, France

[#]Dipartimento di Chimica, Università degli Studi di Perugia, Sezione di Chimica Fisica, via Elce di sotto 8, I-06123 Perugia, Italia

ABSTRACT: Inelastic neutron scattering experiments and molecular dynamics simulations have been used to investigate the low frequency modes, in the region between 0 and 100 meV, of hydration water in selected hydrophilic and hydrophobic biomolecules. The results show changes in the plasticity of the hydrogen-bond network of hydration water molecules depending on the biomolecular site. At 200 K, the measured low frequency density of states of hydration water molecules of hydrophilic peptides is remarkably similar to that of high density amorphous ice, whereas, for hydrophobic biomolecules, it is comparable to that of low density amorphous ice behavior. In both hydrophilic and hydrophobic biomolecules, the high frequency modes show a blue shift of the libration mode as compared to the room temperature data. These results can be related to the density of water molecules around the biological interface, suggesting that the apparent local density of water is larger in a hydrophilic environment

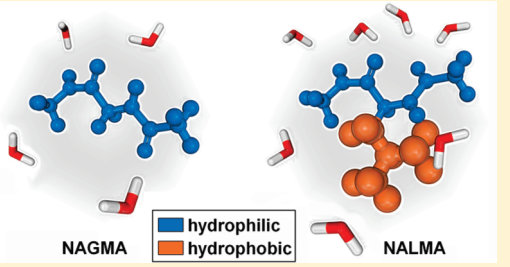

INTRODUCTION

The role of water in the behavior of biomolecules is well recognized.[1−5] In a variety of situations, water molecules not only determine the structure and dynamics of biomolecules, but most biological functions would not take place in their absence. For example, depending on the local environment, a water molecule can form a bridge between adjacent sites fixing an ideal conformation, constitute small pools in hydrophobic regions, hydrate specific chemical groups, activate collective motions, or simply constitute the confined liquid medium with specific acidity and ion concentration. This variety of situations challenges any attempt at a comprehensive description of the behavior of water molecules in biological systems.

The analysis of the vibrational density of states (DOS), in particular the shift and width of the vibrational modes of surface water molecules, constitutes an indirect but rather precise way to differentiate among different situations. It can be obtained accurately from a low energy neutron scattering experiment. The energy of the neutrons in the incident beam is much lower than the thermal energy of water molecules, enabling the evaluation of the DOS at sufficiently small values of the momentum transfer up to the energy of the librational band at 70 meV. The dynamic range extending from the quasi elastic component (∼meV) to 40 meV contains several components identified as intermolecular vibrations, in particular by Raman scattering[6] molecular dynamics[7] and, more recently, by THz absorption.[8] One of these components, the optical mode at 7 meV, is attributed to the fluctuation of the O−O−O angle due to H-bond bending fluctuations. Because it relates to large amplitude motions of hydrogen atoms, it couples very well with neutrons and manifests as a sharp, intense peak better observed by neutron scattering than by Raman scattering.[9,10] Its frequency is also the limiting value of collective motions.[11] Instead, the component at 25 meV, attributed to intermolecular stretching, is barely visible in the neutron spectrum[12] in contrast with Raman scattering or THz absorption.

Quasielastic and low energy inelastic neutron scattering measurements on liquid water and on both crystalline and amorphous ices reveal an intense bending component in the DOS.[13−16] Its position depends very weakly on temperature but is sensitive to intermolecular bonds.[17] In high density amorphous ice (HDA), the peak position is shifted to higher energies as compared to liquid water or low density amorphous ice (LDA).[14] Thus, an analysis of this intermolecular bending component acts as an accurate probe of the environment of water molecules hydrating different sites of a protein.

It has been shown that the low frequency vibrational density of states of protein hydration water at 100 K is similar to the densities of states of high and low density amorphous ice and is

Received: November 4, 2010
Published: March 15, 2011

quite different from that of crystalline ice.[18] The authors correlate the results with the curvature of the protein surface. However, a protein is an example of a heterogeneous surface, which is reflected in the amorphous and heterogeneous structural character of hydration water. Therefore, dynamical and structural measurements only access averaged information, making it impossible to distinguish among contributions from different protein sites, in particular the effects of hydrophobic side chains and of the hydrophilic backbone. The results published by Paciaroni[18] et al. can be considered as an average performed on a complex and heterogeneous system. To understand molecular events in the dynamics of the first hydration shell of a protein, we use simplified protein-model biomolecules, with distinct hydrophilic and hydrophobic properties. In this study, we examine (a) *N*-acetyl-leucine-methylamide (NALMA), which comprises a hydrophobic amino acid side chain, $(CH_3)_2-CH-CH_2$, attached to the C_α atom of a polar blocked polypeptide backbone with CH_3 end-caps, $(CH_3-CO-NH-C_\alpha H-CO-NH-CH_3)$, and (b) *N*-acetyl-glycine-methylamide (NAGMA), which comprises the polar blocked backbone and a hydrogen atom attached to the C_α atom. These two peptides were chosen because their chemical compositions are similar, but NALMA is more hydrophobic than NAGMA because of the hydrophobic leucine side chain.

A number of quasielastic neutron scattering experiments have been performed to study hydrophilic/hydrophobic effects on water dynamics and solute dynamical relaxation for low and high concentrated solutions, from dry to highly hydrated powders. In previous work,[19] we also investigated the effect of temperature and the influence of kosmotropic and chaotropic cosolvents on the hydrogen-bond network dynamics on the hydration water of these biopeptides. In the present work, using small biomolecules that mimic portions of larger biological molecules, we ask how the vibrational modes of hydration water may be affected by the hydrophilic or hydrophobic nature of protein sites rather than by their curvature. We then analyze low temperature inelastic neutron scattering spectra and molecular dynamics simulations of highly hydrated powders of NALMA and NAGMA, to study the dependence on hydrophobicity of hydration water vibrational dynamics, that is, the vibrational density of states. Incoherent neutron scattering probes the vibrational and diffusive motions of the hydrogen atoms, which can be directly simulated by molecular dynamics. The highlight of our work is represented by the experimental investigation performed with the fully deuterated peptides (d-NALMA, d-NAGMA), which enabled a unique study of low frequency vibrational modes of hydration water dynamics at the vicinity of biomolecules with a specific hydrophilic/hydrophobic interface. We find that the vibrational DOS of hydration water molecules surrounding the completely hydrophilic peptide, at 200 K, closely resembles that of high density amorphous ice, whereas the DOS of the hydration water of hydrophobic biomolecules is similar to that of low density amorphous ice. This comparison with the vibrational density of states of the two main forms of amorphous ice, LDA and HDA,[14] yields information about the influence of the hydrophobic properties on water structure and, indirectly, on molecular volumes. Using molecular dynamics (MD) simulation, we characterize the relaxation time for the water−water and water−peptide hydrogen bond (HB) (at the N and O peptide sites, respectively) in the two biomolecules. We find a longer relaxation time in water−water HB around the completely hydrophilic peptide and a very distinct behavior, as a function of biointerface, on the water−peptides HBs relaxation time. Additional MD results show that the densities of states between 50 and 200 K are similar and that at 200 K the differences between the densities of states of NALMA and NAGMA only show up at very high hydration levels, that is, when a HB network is established.

We propose an interpretation of the fact that the DOS of protein hydration water can be well reproduced by a linear combination with equal weight of HDA and LDA.[18]

EXPERIMENTAL SECTION

The inelastic incoherent neutron scattering (INS) experiments were performed at the NIST Center for Neutron Research (NCNR), using the Disk Chopper time-of-flight spectrometer (DCS)[20] with an incident neutron wavelength of 7.5 Å, which corresponds to an elastic wave vector transfer (Q) ranging from 0.15 to 1.57 $Å^{-1}$ and an energy resolution of 35 μeV (correlation time ≈ 40 ps) at full width half-maximum (fwhm). Data were collected at 200 K. In previous published papers, we have already shown the absence of diffusive contributions[19f] and a gradual evolution from librational motion to hindered rotations, for water molecules at this temperature.[19a] Complementary measurements, on the IN6 time-focusing spectrometer at the Institut Laue Langevin, using an incident wavelength of 5 Å, were performed for the hydrated d-NALMA to confirm our results and speculations with a very different resolution. All spectra were corrected for scattering by the sample container, and for relative detector efficiencies. The data were reduced using the NCNR's DAVE software package.[21] The density of states (DOS) was calculated using the following simplified expression:[22]

$$\mathrm{DOS} \cong \frac{\mathrm{d}^2\sigma}{\mathrm{d}\Omega\ \mathrm{d}E_\mathrm{f}} \frac{k_\mathrm{i}}{k_\mathrm{f}} \frac{\omega}{Q^2} \left\{ 1 - \exp\left(-\frac{\hbar\omega}{k_\mathrm{B}T} \right) \right\} \qquad (1)$$

where T is the temperature, k_i and k_f are the initial and final wave vectors, and $(\mathrm{d}^2\sigma)/(\mathrm{d}\Omega\ \mathrm{d}E_\mathrm{f})$ is the double differential neutron scattering cross section per unit solid angle and final energy E_f, which is the quantity measured in an inelastic scattering experiment. The DOS calculation ignores corrections such as for multiphonon and multiple scattering and sums over all Q values. This strategy simplifies the comparison of data treated similarly. To compare different DOSs, all curves are normalized to the integral calculated over the plotted energy range. The first two terms of eq 1 may be identified with the incoherent dynamical structure factor $S(Q,\omega)$, which is related to the time-dependent spatial correlation of an atom with itself, providing information about single-particle ("self") dynamics.[22]

The deuterated d-NALMA and d-NAGMA (CDN Isotopes, Canada) were hydrated by adding a well-controlled amount of pure water (H_2O) after total dehydration achieved by placing the sample under vacuum in the presence of silica salts for at least 2 days.[19] Roughly 250 mg of deuterated peptide was used for each sample. The powders were hydrated at 60% for the d-NALMA-H_2O peptide (7 molecules of water per molecule of peptide) and 50% for the d-NAGMA-H_2O sample (4 molecules of water per molecule of peptide), which corresponds to full hydration in both cases.[19a] The total amount of added hydration water was determined from the change in mass of the samples. Samples were loaded and sealed into slab-shaped aluminum containers of 0.1 mm thickness.

RESULTS AND DISCUSSION

As a preliminary analysis of the measured intensities, dynamical structure factors of hydrated d-NALMA-H_2O and d-NAGMA-H_2O, summed over all scattering angles and normalized by the integral over the whole energy range, are reported in Figure 1a. The data measured at 200 K are compared to those of high density and low density amorphous ice measured at 75 K.[14]

dx.doi.org/10.1021/ja109610f |*J. Am. Chem. Soc.* 2011, 133, 4882–4888

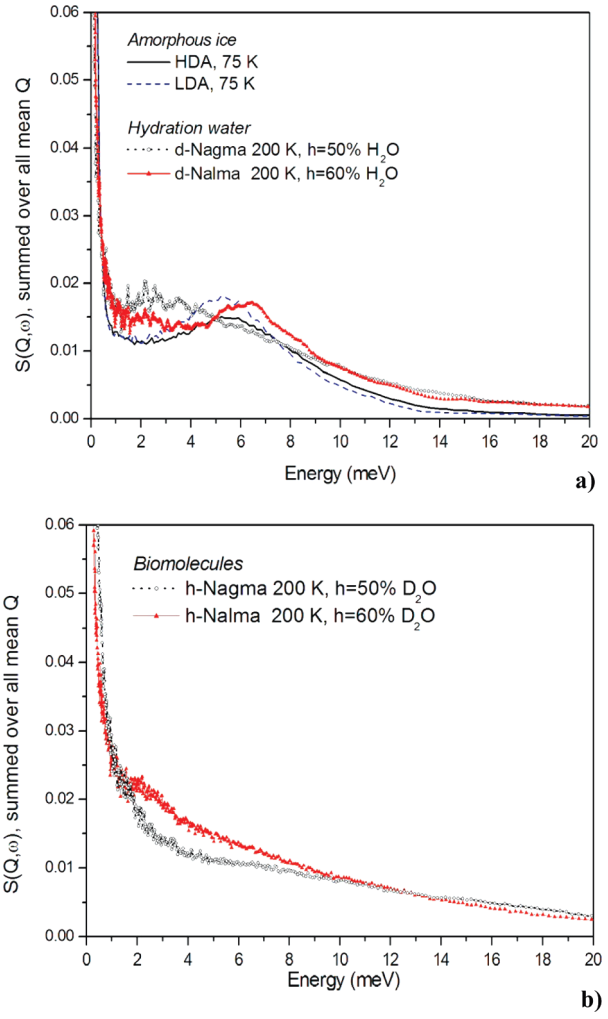

Figure 1. (a) Hydration water: Incoherent scattering function, summed over all Q, for 60% hydrated d-NALMA (▲), 50% hydrated d-NAGMA (○) at 200 K, and HDA ice (—) and LDA ice (– – –) at 75 K.[14] (b) Biomolecules: Incoherent scattering function for 50% hydrated h-NAGMA (○) and 60% hydrated h-NALMA (▲) at 200 K. In this figure and subsequent figures, error bars representing standard deviations, not shown for readability, are commensurate with the scatter of the data points.

The $S(Q,\omega)$ of hydration water of d-NALMA-H_2O (which is largely hydrophobic) shows a distinct and pronounced bump at ~6.3 meV and a weak shoulder between 1 and 4 meV, while d-NAGMA-H_2O (which has a hydrophilic interface) only shows the shoulder. The broad peak at 6 meV, already observed for other systems, has been assigned to O—O—O intermolecular bending motions of the HB network.[23] The shoulder at low frequency can arise from different components (protein contributions coupled with water motions).[24,25] It is not excluded that, under the hypothesis of a wider distribution of water dynamics at the hydrophilic interface, the bump is smeared, merging into the high energy side of the shoulder. In other words, the hydrophilic interface imposes tighter confinement restricting the amplitude of the O—O—O bending motions. In both cases (hydrophilic and hydrophobic environment), the main cause of changes of the water structure and dynamics is changes in hydrogen-bond network and associated distortions and loss of the tetrahedral symmetry of bulk water.

In first approximation, the association with low density amorphous ice shows an interesting similarity with the d-NALMA-H_2O, which reproduces the well-pronounced bump at low energy. In a general comparison with the $S(Q,\omega)$ hydration water dynamics of protein molecules, we see a combination of the fingerprints of hydrophilic and hydrophobic sites. In particular, Paciaroni et al.[18] have shown a distinct mode at 6 meV and a shoulder between 2 and 5 meV for d-MBP-H_2O (MBP is maltose binding protein). The shoulder seems to disappear when, within the approximation that all hydrogens in a protein have the same behavior in the vibrational region, the authors subtract the N—H exchangeable proton contribution from the hydration water spectra. However, in our case, we verified that their assumption does not affect in such a crucial way the shape of $S(Q,\omega)$ at low frequencies for both hydrophilic and hydrophobic samples. Thus, we exclude any contribution from exchangeable protons. In both hydrogenated peptides, hydrated with D_2O, we observe features at low frequency, but they are different for the two biomolecules (Figure 1b). While the hydrogenated h-NALMA-D_2O shows a shoulder between 2 and 4 meV, the h-NAGMA-D_2O is characterized only by a weak bump. The observed distinct features are in agreement with the work of Tarek and co-workers who, through a MD simulation study, were able to dissect the low frequency spectra of RNase globular protein, into contributions from protein backbone, polar exposed side chains, and nonpolar buried side chains.[26]

These first results provide evidence that both low frequency features of hydration water are intrinsic to the water dynamics when affected by hydrophilic (shoulder ~2—4 meV) and/or hydrophobic (enhancement of the mode at 6 meV) interfaces. We associate the low frequency features, at 2—4 meV, with the dynamics of hydrogen bonds present at very low temperatures even when diffusive motions cannot take place.[19]

Figure 2a shows a comparison of the hydration water translational and librational densities of states for d-NALMA-H_2O and d-NAGMA-H_2O hydrated powders at 200 K between 0 and 100 meV. For purposes of comparison, we also show, in Figure 2b, the behavior of the DOS at 300 K.[19f] For both samples, the DOS is dominated by the librational contribution. At lower energies, in both cases, two translational bands can be identified below 40 meV: one sharp peak centered around 6—8 meV and one broad shoulder at ~20—40 meV. In this low frequency region, it is clear that the position and the shape of the bands due to hydration water depend strongly on the nature of the biomolecular interfaces and on temperature. For d-NAGMA-H_2O, the density of states shows a significant broadening and a shift of the first peak position to higher energy, as compared to d-NALMA-H_2O. This result can be interpreted as a consequence of a larger "rigidity" of the HB network for the hydrophilic interface (that of NAGMA) as recently demonstrated for water inside the cavities of β-cyclodextrin.[27] In addition, the amplitude of the shoulder at 20—40 meV also shows significantly higher intensity. It is worth noting that this intermolecular stretching band is barely visible at room temperature in both cases. The enhancement of amplitude observed at low temperature demonstrates a substantial change in intermolecular interactions. We have confidence in this very distinct shape of the DOS at high resolution given that the density of states for the NALMA obtained from a complementary experiment with a poorer resolution (IN6 data not shown) superimposes the profile depicted in Figure 2a.

In the higher energy part of the spectrum (>40 meV), and for both samples, the librational band is shifted to higher energy as

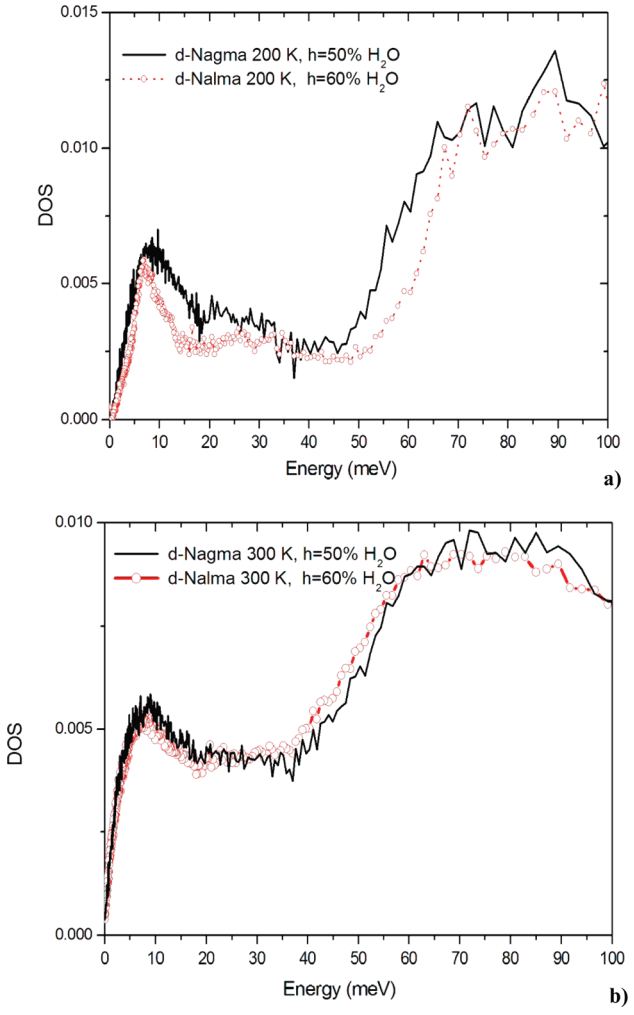

Figure 2. (a) Low energy densities of states of hydration water for 50% hydrated d-NAGMA (—) and 60% hydrated d-NALMA (○) at 200 K. (b) Low energy densities of states of hydration water for 50% hydrated d-NAGMA (○) and 60% hydrated d-NALMA (▲) at 300 K. For comparison purposes, the densities of states were normalized to their integral between 0 and 100 meV.

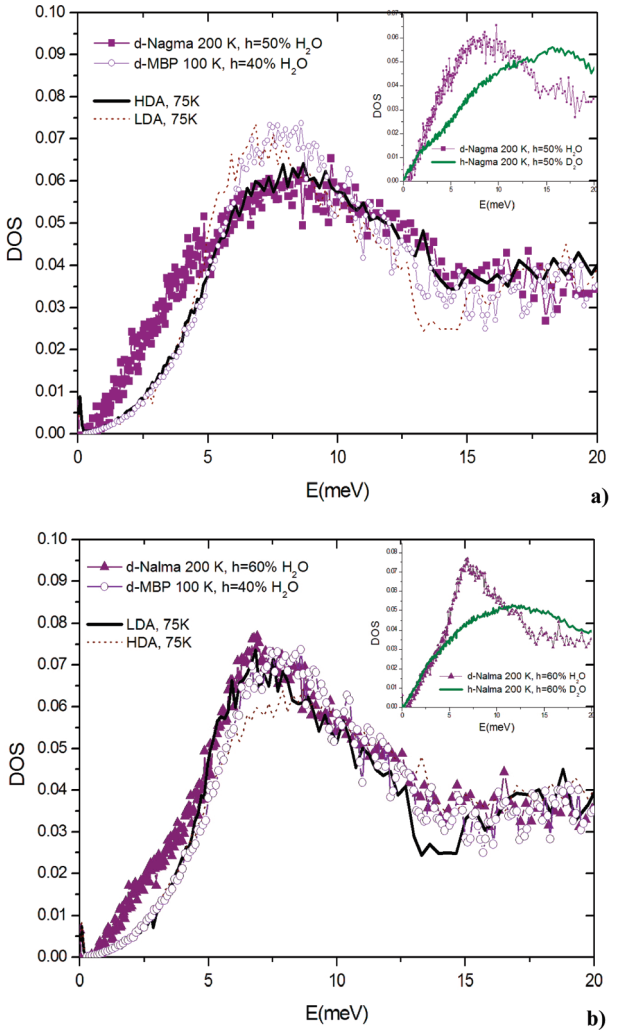

Figure 3. (a) Low energy densities of states of hydration water for 50% hydrated d-NAGMA (■) at 200 K, maltose binding protein at 100 K (○), and the LDA (---) and HDA (—) at 75 K. Inset: DOS of the hydrated peptide h-NAGMA (—) as compared to the d-NAGMA hydration water (■). (b) Low energy densities of states of hydration water for 60% hydrated d-NALMA (▲) at 200 K, maltose binding protein at 100 K (○), and the LDA (—) and HDA (---) at 75 K. Inset: DOS of the hydrated peptide h-NALMA (—) as compared to the d-NAGMA hydration water (▲). For comparison purposes, the densities of states were normalized to their integral between 0 and 20 meV.

compared to 300 K data sets; such a behavior is also observed in supercooled water.[28] More concretely, at 200 K, the band is centered at ~90 meV, whereas it is at ~75 meV at 300 K and its narrower shape is reminiscent of the fingerprint of ice-like dynamics. The comparison of the 200 K spectra for our two samples in the region between 50 and 70 meV shows two distinct profiles where the trend, from NAGMA to NALMA, is similar to the effect due to a lowering of the temperature or hydration level, provoking suppression of the lower frequency modes. The largest effect observed in the hydrophobic case is remarkable because the number of molecules of water around the d-NALMA-H_2O is higher than that around d-NAGMA-H_2O (7 and 4 H_2O molecules, respectively). This trend is closely associated with water network geometry.

To better understand the relation between the measured vibrational frequency bands of water molecules around a protein surface and the hydrophilic and hydrophobic biomolecules site, we compare the low frequency DOS with those of d-MBP-H_2O protein and high and low density amorphous ice.[14,18] Figure 3 represents the low frequency DOS normalized to the integral between 0 and 20 meV for the hydration water around the d-NAGMA-H_2O (a) and d-NALMA-H_2O (b) at 200 K, together with the MBP measured at 100 K[18] and the LDA and HDA at 75 K (all DOSs were obtained following the same procedure). It is worth remembering that we verified with MD simulations that the DOS at 200 K shows exactly the same profile and intensity as at 50 K.

In Figure 3a and b, we observe an "anomalous" behavior of the DOS of NAGMA/NALMA hydration water between 0 and 5 meV when compared to LDA, HDA, and MBP. This same feature also appears in the complementary IN6 neutron scattering data. The observed contribution could arise from modes intrinsic to the peptide itself (DOS of H-peptides-D_2O in the inset of Figure 3a and b), but the low frequency profiles do not resemble each other. We are confident that the effect that we observe is not an artifact of the data but a real mode that could be related to the characteristic

dx.doi.org/10.1021/ja109610f |J. Am. Chem. Soc. 2011, 133, 4882–4888

dynamics of the structure of hydration water at low temperature specific to these interfaces, or to the phonon DOS in these systems, or to a glassy former property of biomolecules, or less likely to a residual quasi-elastic signal. It is worth noting that at room temperature this feature looks quite similar for the two peptides, whereas at low temperature there is a significant difference (Figure 2a and b). To compare our data with those of amorphous ice and protein hydration water, we address our attention to the higher frequency region of the density of states (5−20 meV).

Figure 3a shows that the bending component (at 7.5 meV) of the DOS of hydration water around the completely hydrophilic molecules (NAGMA) coincides with the DOS of HDA. In other words, water molecules at the interface with a homogeneous hydrophilic biomolecule show, at low temperature, a vibrational behavior identical to that of HDA.

Figure 3b shows the larger changes generated by the presence of the hydrophobic side chain, in the NALMA sample. The same peak is now shifted to lower energy (from 7.5 to 6.5 meV), and its intensity increases. It appears superimposed on that of LDA up to 12 meV where it starts to reproduce the HDA vibrational modes. In this comparison, the MBP-H_2O hydration water is very similar to that of d-NALMA-H_2O except for the shift of its main peak, which is justified by the different degree of the surface heterogeneity. These results therefore show that the heterogeneity introduced by the addition of a hydrophobic side chain promotes a vibrational dynamics similar to that of low density amorphous ice. In previous work, we have shown that, because of the heterogeneity of NALMA chemistry, at room temperature and in solution, the dynamics of the first hydration layer is more complex than that observed at the more homogeneous NAGMA backbone.[29]

It is tempting to interpret our results within the context of the evaluation of water density at the vicinity of hydrophobic interfaces. It is generally accepted that water density or, more exactly, the molecular volume is modified in the vicinity of hydrophobic surfaces. On the contrary, the volume occupied by water molecules in the first layer above a hydrophilic substrate is smaller than that in the bulk.[30] Such an effect may be due to the formation of deformed hydrogen bonds between water molecules and the interface along with disruption of the open tetrahedral water structure.

The results that we discussed above show clearly that, for the intermolecular O−O−O bending vibration, the behavior of hydration water is similar to that of HDA in the case of a hydrophilic substrate and similar to that of LDA for the hydrophobic situation. It is tempting to say that the local "density" of water is also higher in the case of a hydrophilic substrate. Another way to interpret the apparently higher density is that the formation of hydrogen bonds between water and the organic substrate drastically changes the local tetrahedral structure, generating a layer where the bonds are very distorted, thus similar to the situation of HDA. In contrast, close to a sufficiently large hydrophobic interface, particularly at low temperature, water molecules generate a relatively stable and open hydrogen-bond network not substantially different from that of LDA and associated with a lower "density". Consequently, with this simple analogy strictly based on the analysis of the vibrational density of states, our results support the idea that the apparent local density of water is greater in a hydrophilic environment. However, this extended interpretation should not be considered as a proof of an increased hydration water density around hydrophilic solutes.

To complete this dynamical picture and to probe the specific behavior of water−water and water−peptides HB relaxation,

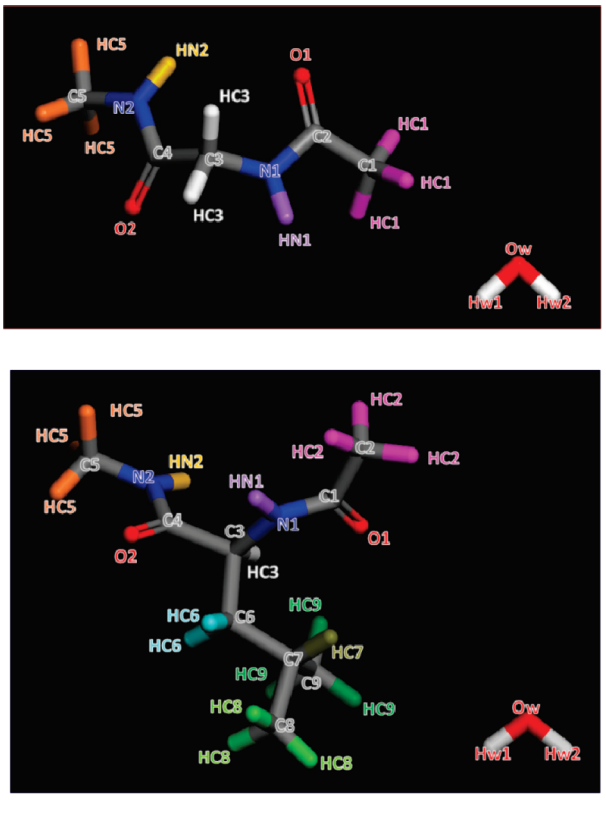

Figure 4. Labeling of the peptide and water atoms used in MD simulations. (a) NAGMA, (b) NALMA.

molecular dynamics simulations are absolutely necessary. We performed MD studies of hydration water under the same experimental conditions (hydration level and temperature). Simulations were performed using the Forcite module provided in Materials Studio 5.0[31] with the COMPASS 27 forcefield.[32] Two simulation boxes containing 100 NAGMA and 400 water molecules and 72 NALMA and 504 water molecules, respectively, were prepared and initially equilibrated in the NVT ensemble during 260 ps with a time step of 1.0 fs, and using Berendsen's thermostat with a relaxation constant of 1.0 ps. Three-dimensional cubic periodic boundary conditions were applied, and a cutoff of 10 Å was employed to compute the van der Waals interactions, while the Ewald summation was used to treat the long-range electrostatic interactions. The equilibration run was followed by a production run of 1 ns performed also in the NVT ensemble and using the same conditions.

To get some statistics with regard to the HB network surrounding, respectively, NAGMA and NALMA peptides, we performed a HB survival analysis based on the following algorithm. First, we identify all the HB formed between acceptor (A) and donor (D) atoms in the system using the following geometric criteria to decide whether an HB was formed: $d_{A-D} \leq 3.5$ Å and $150° \leq \theta_{D-H\cdots A} \leq 180°$. The HB lifetime distribution is then obtained by counting for each detected HB how long it lasts. In that context, it should be mentioned that a given HB that was formed once, then broken and reformed later, was treated as two independent HBs. This computation is equivalent to that of Luzar as the survival probability for a newly generated bond.[33] The HB relaxation time could then be obtained by fitting the long time behavior of the survival probability to an exponential.

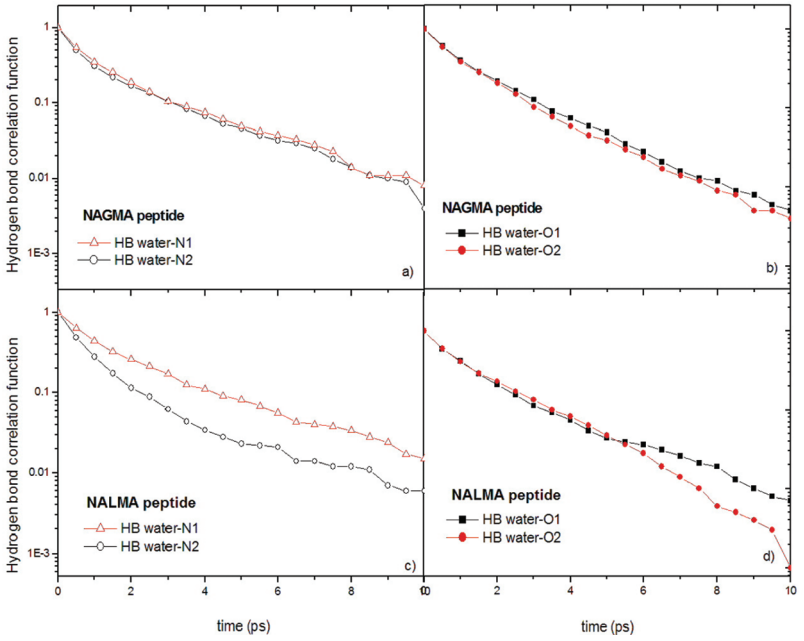

Figure 5. Hydrogen-bond correlation function inferred from MD trajectory and calculated up to 10 ps for the water-bonded NAGMA peptide (a,b) and NALMA peptide (c,d) at the donor nitrogen (N_1, N_2) and acceptor oxygen (O_1, O_2) binding sites.

Here, we report some results that are relevant to our neutron data. One of the highlights of our results is the ability to label all of the atoms in the molecule and to analyze the HB relaxation time in specific donor and acceptor binding sites, that is, N_1, N_2, O_1, O_2 (where N_1 and O_2 are the closest C_α—nitrogen and oxygen atoms on the peptide backbone) as shown in Figure 4.

Figure 5 shows the hydrogen-bond survival probability for water molecules bonded to NAGMA (a,b) and NALMA (c, d) at the nitrogen (N_1, N_2) and oxygen (O_1, O_2) binding sites. There is a marked difference in the time dependence of the established hydrogen bonds between the two different interfaces. In the completely hydrophilic case (that of NAGMA), there is no distinction between the two sets of sites (N_1, N_2) and (O_1, O_2), and the inferred characteristic time is of ~2.5 ps for the N-sites and ~1.9 ps for the O-sites. However, the presence of an extended hydrophobic chain, attached to the C_α carbon, in the NALMA peptide is strongly reflected in N_1 and N_2 hydrogen-bonding relaxation time (Figure 5c) measured as ~2.8 and ~1.8 ps, respectively. A less pronounced, but still visible, effect is observed at the oxygen's HB binding sites (~1.6 and ~2 ps). This "faster" dynamics effect in the NALMA hydration water is also confirmed by the water—water HB, which we found to be 2.7 ps for NALMA and 3.2 ps for the NAGMA.

Together with the DOS results, it seems then quite straightforward to conclude that water molecules close to the chains reorient faster because of a different binding geometry and/or density of the water network as compared to those around the completely hydrophilic interface. Thus, our results point to the existence of an open structure of tetrahedral arranged hydrogen-bonded water molecules with four nearest neighbors as in LDA for the hydrophobic interface and a mixture of "constrained frozen bonds" as in HDA for the hydrophilic one.

CONCLUSIONS

Our work contributes to assigning the specific contribution of the distinct sites to the polymorphism state of protein hydration water at low temperature. We find that the similarity with amorphous ice behavior is not due to the protein's curvature but arises from the particular characteristics of the amino acids. We proved that hydrophilic sites enhance high density amorphous ice vibrational behavior, while hydrophobic sites promote the low density amorphous ice vibrational dynamics. Together with support from MD simulations, we interpreted this signature as the fact that the density of water around the biological interface is higher around hydrophilic than around hydrophobic sites.

AUTHOR INFORMATION

Corresponding Author
russo@ill.fr

ACKNOWLEDGMENT

D.R. thanks ILL and NIST for beam time allocation, and A. Paciaroni and M. Koza for kindly providing their data for comparison. This work utilized facilities supported in part by the National Science Foundation under Agreement No. DMR-0454672. A materials supplier is identified in this Article to foster understanding. Such identification does not imply recommendation or endorsement by the National Institute of Standards and Technology, nor does it imply that the materials identified are necessarily the best available for the purpose.

REFERENCES

(1) Bagchi, B. *Chem. Rev.* **2005**, *105*, 3197.
(2) (a) Modig, K.; Qvist, J.; Marshall, C.; Davies, P. L.; Halle, B. *Phys. Chem. Chem. Phys.* **2010**, *12*, 10189. (b) Sunde, E. P.; Setlow, P.; Hederstedt, L.; Halle, B. *Proc. Natl. Acad. Sci. U.S.A.* **2009**, *106*, 19334.

(3) Chaplin, M. *Nat. Rev. Mol. Cell Biol.* **2006**, *7*, 861.
(4) Ball, P. *ChemPhysChem* **2008**, *9*, 2677.
(5) (a) Doster, W. *Biochim. Biophys. Acta* **2010**, *1804*, 3. (b) Doster, W.; Busch, S.; Gaspar, A. M.; Wuttke, M. S. J.; Scheer, H. *Phys. Rev. Lett.* **2010**, *104*, 098101.
(6) Bansil, R.; Wiafe-Akenten, J.; Taaffe, J. L. *J. Chem. Phys.* **1982**, *76*, 2221.
(7) Corongiu, G.; Clementi, E. *J. Chem. Phys.* **1992**, *98*, 4984.
(8) Heyden, M.; Sun, J.; Funkner, S.; Mathias, G.; Forbert, H.; Havenith, M.; Marx, D. *Proc. Natl. Acad. Sci. U.S.A.* **2010**, *107*, 12068.
(9) Krushnamurthy, S.; Bansil, R.; Wiafeakenten, J. *J. Chem. Phys.* **1983**, *79*, 5863.
(10) Walrafen, G. E. *J. Phys. Chem.* **1990**, *94*, 2237.
(11) Teixeira, J.; Bellissent-Funel, M. C.; Chen, S. H.; Dorner, B. *Phys. Rev. Lett.* **1985**, *54*, 2681.
(12) Settles, M.; Doster, W. *Faraday Discuss.* **1996**, *103*, 269.
(13) (a) Teixeira, J.; Bellissent-Funel, M.-C.; Chen, S. H.; Dianoux, A. J. *Phys. Rev. A* **1985**, *31*, 1913. (b) Bellissent-Funel, M. C.; Texeira, J. *J. Mol. Struct.* **1991**, *250*, 213.
(14) Koza, M. M.; Geil, B.; Winkel, K.; Kohler, C.; Czeschka, F.; Scheuermann, M.; Schober, H.; Hansem, T. *Phys. Rev. Lett.* **2005**, *94*, 125506.
(15) Kolesnikov, A. I.; Li, J.; Parker, S. F.; Eccleston, R. S.; Loong, C. K. *Phys. Rev. B* **1999**, *59*, 3569.
(16) Kolesnikov, A. I.; Sinitsyn, V. V.; Ponyatovsky, E. G.; Natkaniec, I.; Smirnov, L. S. *J. Phys.: Condens. Matter* **1994**, *6*, 375.
(17) Toukan, K.; Rahman, A. *Phys. Rev. B* **1985**, *31*, 2643.
(18) Paciaroni, A.; Orecchini, A.; Cornicchi, E.; Marconi, M.; Petrillo, C.; Haertlein, M.; Moulin, M.; Schober, H.; Tarek, M.; Sacchetti, F. *Phys. Rev. Lett.* **2008**, *101*, 148104.
(19) (a) Russo, D.; Ollivier, J.; Teixeira, J. *Phys. Chem. Chem. Phys.* **2008**, *10*, 4968. (b) Russo, D.; Baglioni, P.; Peroni, E.; Teixeira, J. *Chem. Phys.* **2003**, *292*, 235. (c) Russo, D.; Hura, G.; Copley, J. R. D. *Phys. Rev. E* **2007**, *75*, 1. (d) Russo, D.; Teixeira, J.; Ollivier, J. *J. Chem. Phys.* **2009**, *130*, 235101. (e) Russo, D. *Chem. Phys.* **2008**, *345*, 200. (f) Russo, D.; Copley, J. R. D.; Ollivier, J.; Teixeira, J. *J. Mol. Struct.* **2010**, *972*, 81.
(20) Copley, J. R. D.; Cook, J. C. *Chem. Phys.* **2003**, *292*, 477.
(21) Azuah, R. T.; Kneller, L. R.; Qiu, Y.; Tregenna-Piggott, P. L. W.; Brown, C. M.; Copley, J. R. D.; Dimeo, R. M. *J. Res. Natl. Inst. Stand. Technol.* **2009**, *114*, 341.
(22) Squires, G. L. *Introduction to the Theory of Thermal Neutron Scattering*; Cambridge University Press: Cambridge, UK, 1978; Chapter 3.
(23) Walrafen, G. E. *J. Chem. Phys.* **1964**, *40*, 3249.
(24) Tarek, M.; Tobias, D. J. *Phys. Rev. Lett.* **2002**, *89*, 275501.
(25) Settles, M.; Doster, W. *Faraday Discuss.* **1996**, *103*, 269.
(26) Tarek, M.; Tobias, D. J. *J. Chem. Phys.* **2001**, *115*, 1607.
(27) Jana, M.; Bandyopadhyay, S. *Langmuir* **2010**, *26*, 14097.
(28) Chen, S. H.; Toukan, K.; Loong, C. k.; Price, D. L.; Teixeira, J. *Phys. Rev. Lett.* **1984**, *53*, 1360.
(29) Russo, D.; Hura, G.; Head-Gordon, T. *Biophys. J.* **2004**, *86*, 1852. Russo, D.; Murarka, R. K.; Hura, G.; Verschell, E.; Copley, J. R. D.; Head-Gordon, T. *J. Phys. Chem. B* **2004**, *108*, 19885. Russo, D.; Murarka, R. K.; Copley, J. R. D.; Head-Gordon, T. *J. Phys. Chem. B* **2005**, *109*, 12966.
(30) Helmy, R.; Kazakevich, Y.; Ni, C.; Fadeev, A. Y. *J. Am. Chem. Soc.* **2005**, *127*, 12446.
(31) *Materials Studio Modelling Environment v. 5.0*; Accelrys Inc.: San Diego, CA, 2009.
(32) Sun, H. *J. Phys. Chem. B* **1998**, *102*, 7338.
(33) Luzar, A. *J. Chem. Phys.* **2000**, *113*, 10663.